IOPscience iopscience.iop.org

Home Search Collections Journals About Contact us My IOPscience

Emergence of chaotic behaviour in linearly stable systems

This article has been downloaded from IOPscience. Please scroll down to see the full text article.

2002 J. Phys. A: Math. Gen. 35 499

(http://iopscience.iop.org/0305-4470/35/3/304)

View the table of contents for this issue, or go to the journal homepage for more

Download details:
IP Address: 171.66.16.107
The article was downloaded on 02/06/2010 at 10:16

Please note that terms and conditions apply.

INSTITUTE OF PHYSICS PUBLISHING JOURNAL OF PHYSICS A: MATHEMATICAL AND GENERAL

J. Phys. A: Math. Gen. **35** (2002) 499–516 PII: S0305-4470(02)21883-1

Emergence of chaotic behaviour in linearly stable systems

F Ginelli[1,2], **R Livi**[1,2] **and A Politi**[2,3]

[1] Dipartimento di Fisica, Università di Firenze, Largo E Fermi 2, I-50125 Firenze, Italy
[2] Istituto Nazionale di Fisica della Materia, Unità di Firenze, Largo E Fermi 2, I-50125 Firenze, Italy
[3] Istituto Nazionale di Ottica Applicata, Largo E Fermi 6, Firenze, I-50125 Italy

Received 7 February 2001, in final form 30 October 2001
Published 11 January 2002
Online at stacks.iop.org/JPhysA/35/499

Abstract

Strong nonlinear effects combined with diffusive coupling may give rise to unpredictable evolution in spatially extended deterministic dynamical systems even in the presence of a fully negative spectrum of Lyapunov exponents. This regime, denoted as 'stable chaos', has been so far mainly characterized by means of numerical studies. In this paper we investigate the mechanisms that are at the basis of this form of unpredictable evolution generated by a nonlinear information flow through the boundaries. In order to clarify how linear stability can coexist with nonlinear instability, we construct a suitable stochastic model. In the absence of spatial coupling, the model does not reveal the existence of any self-sustained chaotic phase. Nevertheless, already this simple regime reveals peculiar differences between the behaviour of finite-size and that of infinitesimal perturbations. A mean-field analysis of the spatially extended case provides a semi-quantitative description of the onset of irregular behaviour. Possible relations with directed percolation as a synchronization transition are also briefly discussed.

PACS number: 05.45+b

1. Introduction

Unpredictable evolution in dynamical systems is due to the propagation of information. For instance, the sensitivity of trajectories to infinitesimal perturbations means that any arbitrarily small inaccuracy about the initial conditions is exponentially amplified in time, with an average rate associated with the maximum Lyapunov exponent. The integral of the positive component of the whole Lyapunov spectrum, the so-called Kolmogorov–Sinai entropy [1], measures the production rate of information that flows from the less to the more significant digits of the dynamical variables. In particular, the existence of at least one positive Lyapunov exponent is

 © 2002 IOP Publishing Ltd Printed in the UK

a sufficient condition for identifying chaotic dynamics; conversely, a fully negative spectrum implies a periodic evolution.

The approach to unpredictable evolution based on linear stability analysis has been developed for finite (low-dimensional) systems. Its extension to spatially extended dynamical systems is based on the implicit assumption that they can be viewed as a collection of almost independent, finite-dimensional subsystems. The existence of a limit Lyapunov spectrum [2, 3] provides strong support to this hypothesis and typical chaoticity indicators, such as entropies and generalized dimensions, can be turned into their corresponding densities [4]. In fact, a primary interest in the study of spacetime chaos is the identification of thermodynamic-like properties.

However, Lyapunov instability is not the only source of unpredictability in such systems. Actually, information can also flow through the boundaries and be transmitted in space by non-linear mechanisms of front propagation. The so-called chaotic rules of deterministic cellular automata (DCA) [5] are typical examples of unpredictable evolution in the absence of linear instabilities. There, each variable can take only a finite number, s, of discrete states. This prevents the very existence of infinitesimal perturbations, while, on the other hand, even isolated 'state-flips' may propagate through the lattice with finite velocity, giving rise to irregular dynamics. In fact, any DCA rule defined over a lattice of L cells is bounded to exhibit a periodic behaviour since the number of possible states is s^L. What makes a 'chaotic' DCA rule different from an ordered one is the exponential growth with L of the recurrence time of the typical configurations. Accordingly, the unpredictable behaviour is dynamically persistent only in the infinite-size limit, $L \to \infty$.

A very similar unpredictable behaviour, denoted as *stable chaos*, has also been observed in coupled map lattice (CML) models [6, 8] of the following type:

$$x_i(t+1) = f\left(\frac{\varepsilon}{2}x_{i-1}(t) + (1-\varepsilon)x_i(t) + \frac{\varepsilon}{2}x_{i+1}(t)\right) \tag{1}$$

where $x_i(t)$ is the continuous state variable at time t on site i of a one-dimensional lattice; the function f is a linearly stable map of the interval [0, 1] into itself and ε is the strength of the diffusive coupling. It is worth pointing out that this spatial coupling cannot produce any linear instability mechanism and the whole spectrum of Lyapunov exponents is found to be negative. Accordingly, the CML dynamics must eventually approach a periodic stable attractor. This notwithstanding, if f is equipped with a sufficiently strong non-linearity (e.g. a discontinuity or a region with rapidly varying slope), one can identify a region in parameter space, where the 'transient' evolution towards the periodic attractor is characterized by unexpected features: space and time correlation functions decay exponentially, as in standard chaotic dynamics, while observables rapidly approach stationary average values. In particular, despite the irregular character of stable chaos, a steady contraction rate of trajectories is obtained after a few timesteps.

Many independent numerical studies (see, e.g., [7, 8]) confirm that, analogously to DCA chaotic rules, the average transient time in this dynamical regime grows exponentially with L. Accordingly, the eventual periodic attractor has no practical relevance in the thermodynamic limit.

A careful inspection indicates that the mechanism of information production in stable chaos is a flow from the outer (left and right) parts of the chain, as in chaotic DCA rules [8]. Accordingly, the unpredictability of stable chaos relies upon a genuine non-linear propagation mechanism. This is why stable chaotic evolution can be efficiently detected by *damage spreading* analysis, i.e. by verifying that an initially perturbed region in space spreads with

a finite front velocity. As discussed in [8], this velocity can be interpreted as a sort of generalization of the standard Lyapunov exponent.

Numerical studies of stable chaos have contributed to shed some light on the relationship between this dynamical regime and the appearance of many interesting complex phenomena, such as non-equilibrium phase transitions, spiral chaos and the propagation of rough interfaces [9–11]. However, little is known about the basic mechanisms yielding stable chaos. In this paper we aim to make some progress in this direction, by investigating the conditions under which finite amplitude perturbations can spread with a finite velocity.

In analogy with various analytical techniques introduced for estimating the maximum Lyapunov exponent in standard chaotic CMLs [12, 13], we assume that a stable chaotic evolution generates a truly random pattern in phase-space, characterized by short range correlation. Thereby, we introduce a suitable stochastic model, describing the evolution in the difference space. Besides diffusion, the model dynamics allows for a random alternation of contraction and expansion processes, the probability of which depends on the size of the perturbation. In section 2 we verify that the stochastic model, with an appropriate choice of the parameter values, is able to reproduce, not only qualitatively but also quantitatively, the main features of stable chaos. Afterwards, while keeping the key ingredients of the model untouched, we further simplify the stochastic rule to obtain an analytical treatment.

In order to understand how a finite perturbation can be sustained even in the presence of an average contraction rate, we first discuss the uncoupled, i.e. zero-dimensional, case in section 3, where propagation of perturbations is absent by definition. The negative Lyapunov exponent obviously implies that perturbations are eventually absorbed, so that stable chaos cannot exist in this framework. Nonetheless, the presence of a non-uniform contraction process yields non-trivial properties of the dynamics. They are exemplified by the difference existing between the standard multifractal spectrum (associated with infinitesimal perturbations) and the spectrum defined in this paper to describe the evolution of finite perturbations. In fact, a noteworthy result of section 3 is that it is possible to define a finite-size multifractal spectrum, independent of the initial amplitude of the perturbation.

The methods and concepts introduced in section 3 are applied in section 4 to the study of the spatially extended version of the stochastic model. For lack of space we limit our discussion to the case of 'democratic' coupling, but it is clear that stable chaos arises in a broad region of strong coupling. It is precisely the diffusive coupling which is responsible for the sustainment of stable chaos. Over small scales, contraction is more effective than the sporadic amplification: in such circumstances, diffusion just levels the damping process. Conversely, at larger scales, diffusion proves to be an effective mechanism to propagate locally generated amplifications. The net effect is that, in suitable parameter regions, perturbations self-sustain.

By introducing a factorization hypothesis of the spatial degrees of freedom, we obtain a good estimate of the probability distribution associated with the spatially extended dynamics. In particular, we find a critical value of the contraction rate separating an ordered regime, where any perturbation eventually vanishes, from a chaotic regime, where the average value of the perturbation remains finite in the infinite time limit. A mean-field argument provides a fairly accurate description of the overall scenario.

The transition exhibited by the stochastic model is reminiscent of the 'fuzzy' transition region found in a deterministic CML [14]. However, the analogy cannot be extended to a quantitative level, since the chaotic CML dynamics is self-generated and thus it is increasingly regular when the transition region is approached (this is the main reason for the fuzziness observed in [14]); conversely, here the stochastic properties of the contraction/expansion process are fixed *a priori*. A tight analogy, instead, exists with the stochastic synchronization

induced by an additive noise [15]. Indeed, in this context, the external noise does not change its robust stochastic features when passing from the synchronized to nonsynchronized regime. It is precisely this analogy which suggests that the transition described in this paper should belong to the universality class of directed percolation [16]. The numerical simulations described in section 5 do confirm such an expectation, but subtle problems still prevent us from drawing definite conclusions. Such open problems and the possible future perspectives are summarized in section 5.

2. Generalities

The typical functions used to investigate stable chaos in CML are piecewise linear maps of the unit interval of the following form:

$$f(x) = \begin{cases} c_1 x & 0 \leqslant x < 1/c_1 \\ 1 - (x - 1/c_1)(1 - c_2)/\Delta & 1/c_1 \leqslant x < 1/c_1 + \Delta \\ c_2 + c_3[x - (1/c_1 + \Delta)] & 1/c_1 + \Delta \leqslant x \leqslant 1 \end{cases} . \tag{2}$$

The most studied case in the literature [8] corresponds to the limit $\Delta \to 0$, where $f(x)$ reduces to a discontinuous function. As we shall comment in this paper, a strongly non-linear branch of map $f(x)$, rather than a true discontinuity, is sufficient to yield stable chaos. This is why we prefer to consider here the more general case (2). In the parameter range of interest for the present study, all initial conditions (except for a set of zero Lebesgue measure) converge to the same periodic orbit. For instance, choosing $c_1 = 2.7$, $c_2 = 0.07$, $c_3 = 0.1$ and $\Delta = 0.01$, this is a stable period-3 orbit with Lyapunov exponent $\lambda_0 = -0.316\ldots$.

In a range of values of the diffusive coupling parameter ϵ (see equation (1)), this CML dynamics exhibits a 'chaotic' evolution, despite the largest Lyapunov exponent being kept negative. As already mentioned in the introduction, damage spreading analysis provides a first hint about the mechanism that is responsible for the sustainment of such irregular dynamics. More precisely, stable chaos is generated by a flow of information from the outer (left and right) to the inner regions of an infinite chain, at variance with standard chaos, that amounts to a flow of information from the less to the more significant digits. The latter flow can be 'easily' studied thanks to the linearity of the process (in fact, over sufficiently small scales, any smooth function can be linearized); unfortunately, the same argument does not apply to the dynamics at the left and right edges, that is equally non-linear at any spatial position.

This is the main reason for the difficulty in deriving the necessary and sufficient conditions for the propagation of perturbations. Moreover, while the dynamics of an infinitesimal perturbation can be studied by neglecting propagation phenomena, the opposite is not possible. One cannot study propagation without properly accounting for the local contraction/expansion mechanisms.

The damage spreading analysis is performed by studying the dynamical variable $u_i(t) = |x_i(t) - y_i(t)|$, i.e. the absolute value of the difference between two test trajectories, $x_i(t)$ and $y_i(t)$, that are initially set equal to one another on the right of some lattice site, while they are assumed to be totally independent on the left. With such a setting, the damage spreading analysis amounts to studying the propagation of a front, separating the region in space where $u_i(t) \sim \mathcal{O}(1)$ (the tail) from the region where the two trajectories converge to each other, $u_i(t) \sim 0$ (the forefront).

The first conceptual problem that we have to face is not just the propagation of the front, but its self-sustainment in spite of the local average contraction rate. In order to shed some light on this crucial point, we have simplified the model by assuming that the dynamics is indeed irregular, thereby determining whether this assumption is consistent with the sustainment of an

$\mathcal{O}(1)$ perturbation. This is analogous to the consistency approach developed for the description of standard chaos, where complete randomness of the multipliers of the evolution operator in the tangent space is assumed in order to estimate the maximum Lyapunov exponent [12, 13].

Accordingly, we introduce a suitable stochastic model to describe the evolution in the 'difference' space spanned by $u_i(t)$. Let us start from the simple case $\Delta = 0$. With reference to the CML dynamics, the dynamical rule is composed of two steps. The first one corresponds to the application of the standard discrete diffusive operator

$$\tilde{u}_i(t) = (1-\varepsilon)u_i(t) + \frac{\varepsilon}{2}u_{i+1}(t) + \frac{\varepsilon}{2}u_{i-1}(t) \tag{3}$$

where $0 \leqslant \epsilon \leqslant 1$ is the coupling parameter. The second step contains the stochastic component of the evolution rule,

$$u_i(t+1) = \begin{cases} r_i(t+1) & \text{w.p.} \quad p = \min[1, b\tilde{u}_i(t)] \\ a\tilde{u}_i(t) & \text{w.p.} \quad 1-p \end{cases} \tag{4}$$

where 'w.p.' is the shorthand notation for 'with probability'. The last equation is devised in order to simulate the evolution of $u_i(t)$ in the CML dynamics. Whenever $x_i(t)$ and $y_i(t)$ lie on the same side of the map-discontinuity, their distance is typically contracted: this is schematized by the second line in equation (4), where, for the sake of simplicity, we assume a constant contraction factor $a \in (0, 1)$. In fact, numerical studies of models with constant slope [6] have revealed similar phenomena and we are here interested in capturing the essence of the underlying mechanisms. Alternatively, a sudden amplification occurs to a value, $r_i(t+1) \sim \mathcal{O}(1)$, that is determined in the CML dynamics not only by the difference, $u_i(t)$ between the two orbits, $x_i(t)$ and $y_i(t)$, but also by their actual values. As this latter information is missing in the difference space, we assume r_i to be distributed according to some probability density $R(u_i, r_i)$, that can be determined *a posteriori* by iterating the CML model. Finally, since an amplification occurs in CML only when $x_i(t)$ and $y_i(t)$ lie on opposite sides of the discontinuity, it is reasonable to conjecture that the jump probability is proportional to the size $u_i(t)$ of the perturbation. The reason for our slightly involved definition, $p = \min[1, b\tilde{u}_i(t)]$, is to ensure that $p \leqslant 1$, independently of the choice for the real parameter b.

Such a stochastic model can be straightforwardly generalized to cover the case corresponding to a CML dynamics with a non-zero Δ. The main difference is that, whenever $\tilde{u}$ is smaller than Δ, u is expanded by a fixed factor Δ^{-1} with a constant probability $b\Delta$, while the previous stochastic rule still applies for $\tilde{u} > \Delta$. This amounts to assuming that only perturbations larger than Δ perceive the steep branch of the map as an effective discontinuity. Accordingly, equation (4) is replaced by

$$\begin{aligned} u_i(t+1) &= \begin{cases} r_i(t) & \text{w.p.} \quad p = \min[1, b\tilde{u}_i(t)] \\ a\tilde{u}_i(t) & \text{w.p.} \quad 1-p \end{cases} && \text{if} \quad \tilde{u}_i(t) > \Delta \\ u_i(t+1) &= \begin{cases} \tilde{u}(t)\delta/\Delta & \text{w.p.} \quad p = b\Delta \\ a\tilde{u}_i(t) & \text{w.p.} \quad 1-p \end{cases} && \text{if} \quad \tilde{u}_i(t) \leqslant \Delta. \end{aligned} \tag{5}$$

One can easily check that these formulae reduce to equation (4) in the limit $\Delta \to 0$.

The maximum Lyapunov exponent of the CML dynamics corresponds to the time average of the expansion rates of infinitesimal perturbations. Also in the context of the stochastic model, one can naturally introduce and define a 'maximum Lyapunov exponent' as

$$\lambda_0 = \lim_{t\to\infty} \lim_{||\boldsymbol{u}(0)||\to 0} \frac{1}{t} \sum_{\tau=0}^{t-1} \ln \frac{||\boldsymbol{u}(\tau+1)||}{||\boldsymbol{u}(\tau)||} = \lim_{t\to\infty} \lim_{||\boldsymbol{u}(0)||\to 0} \frac{1}{t} \ln \frac{||\boldsymbol{u}(t)||}{||\boldsymbol{u}(0)||} \tag{6}$$

where $||\boldsymbol{u}||$ represents the norm of the state vector $\boldsymbol{u} = (u_1, u_2, \ldots, u_L)$.

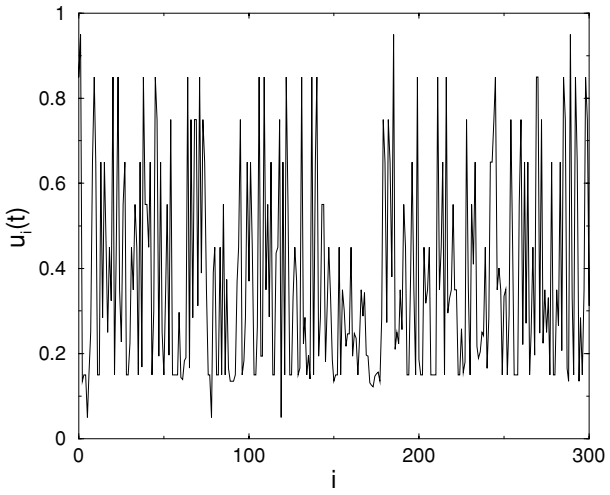

Figure 1. Snapshot of the perturbation profile in the chaotic phase of the stochastic model (3), (5) at time $t = 500$.

An analytic estimate of λ_0 can be obtained by a mean-field argument, according to which the probability of applying the expansion factor $1/\Delta$ is $b\Delta$, while the probability of applying the contraction factor a is $1 - b\Delta$. One easily obtains

$$\lambda_0 \approx b\Delta \ln\left(\frac{1}{\Delta}\right) + (1 - b\Delta)\ln a = \ln a - b\Delta \ln(a\Delta). \tag{7}$$

Numerical simulations indicate that the true value of λ_0 is generally slightly larger than this mean-field estimate.

Moreover, for $\Delta = 0$, $\lambda_0 = \ln a < 0$, while for increasing values of Δ it may become positive, indicating that a standard chaotic regime is attained[4]. Here, we are interested in studying only the parameter region where λ_0 remains negative.

2.1. Comparison between stochastic and deterministic models

Numerical simulations of equation (3) complemented by either rule (4) or (5) have revealed the same qualitative features of the CML dynamics (1) and (2). In particular, when the contraction factor is relatively strong, any initial perturbation $\boldsymbol{u}(0)$ is quickly absorbed to the fixed point $\boldsymbol{u} = 0$; this regime corresponds to the 'ordered' or, equivalently, 'synchronized' phase. On the other hand, for weaker contractions a stable chaotic regime sets in over a time t that grows exponentially with the system size L; in this regime almost any initial condition evolves towards irregular spatial structures, such as the one shown in figure 1. In order to study this process we introduce the single-site probability distribution $Q(t, v)$ of finding a perturbation u in between v and $v + dv$ at time t. Under the assumption of having already taken the limit $L \to \infty$, $Q(t, v)$ approaches quite rapidly a stationary shape $Q(v)$. Accordingly, there exists a limit value

$$u^* = \lim_{t\to\infty} \lim_{L\to\infty} \bar{u}_L(t) \tag{8}$$

[4] This is not entirely correct, since, as discussed in [17], the standard chaotic regime occurs when a stronger constraint is met: the linear propagation velocity coincides with the non-linear one.

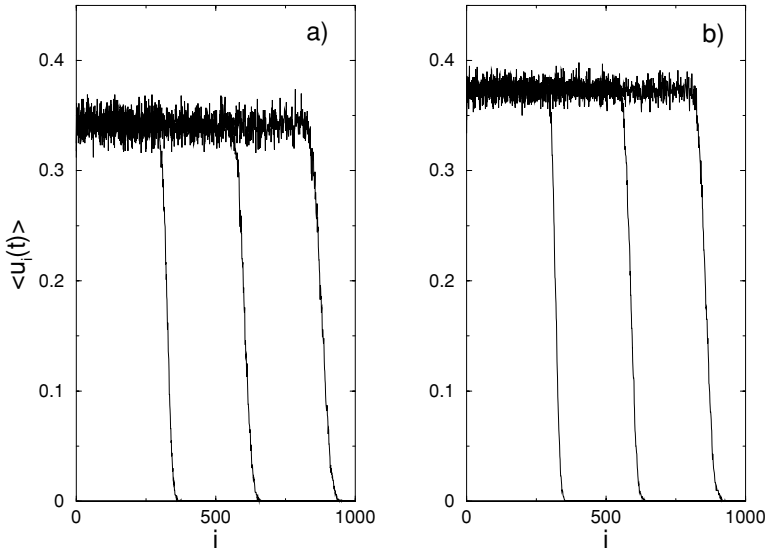

Figure 2. Average front profiles at three different times, t =500, $t = 1000$ and $t = 1500$. Panel (a) refers to the deterministic CML model (1), (2), with parameter values c_1= 2.7, c_2= 0.07, $c_3 = 0.1$, $\Delta = 0$, $\epsilon = 2/3$; averages have been performed over 10^3 initial conditions. Panel (b) refers to the stochastic model (3), (4), with parameter values $a = 0.9$, $b = 1.7$, $\Delta = 0$, $\epsilon = 2/3$; averages have been performed over 10^3 realizations and the probability density $R(u_i, r_i)$ has been sampled over ten channels.

where $\bar{u}_L(t) = \frac{1}{L}\sum_{i=1}^{L} u_i(t)$. u^* plays the role of an order parameter, since it is larger than zero in the chaotic phase, while it is equal to zero in the ordered one.

A better understanding of the stable chaotic phase can be obtained by investigating damage spreading phenomena. For this purpose we consider a 'kink-like' initial condition of the form $u_i(0) = 0$ for $i > L/2$ and $u_i(0)$ equal to a random number uniformly distributed in the interval [0,1] for $i \leqslant L/2$. Additionally, no-flux conditions (i.e. $u_0(t) = u_1(t)$ and $u_L(t) = u_{L+1}(t)$) are imposed at the boundaries, as they do not induce instabilities in the forefront of the perturbation and are reasonably harmless in the chaotic phase.

In the chaotic phase, the initial 'kink-like' structure persists: the front connecting the perturbed with the synchronized region moves with a fluctuating velocity. In order to get rid of the statistical fluctuations affecting each profile, $u_i(t)$ has been smoothed out by performing an ensemble average (over different realizations of the stochastic process) to determine $\langle u_i \rangle$. The average profiles corresponding to three different times are plotted in figure 2(b) for the case $\Delta = 0$. They can be compared with the analogous quantities obtained for the corresponding CML model (see figure 2(a)) where ensemble averages are performed over different initial conditions. Similar pictures are observed for $\Delta \neq 0$.

Several observations are in order. First, we notice that the average front connecting the unperturbed ($u = 0$) with the chaotic ($\langle u_i \rangle = u^*$) regime moves with a constant linear velocity v_F, and that tuning the model parameters, it is possible to find a reasonable agreement with the CML data. Morover, we observe that the width $w(t)$ of the average front profile, defined as the distance between the rightmost sites where $\langle u_i(t) \rangle$ is larger than 0.8 u^* and 0.2 u^*, respectively, exhibits a nearly square-root growth in both the CML and the stochastic models (see figure 3).

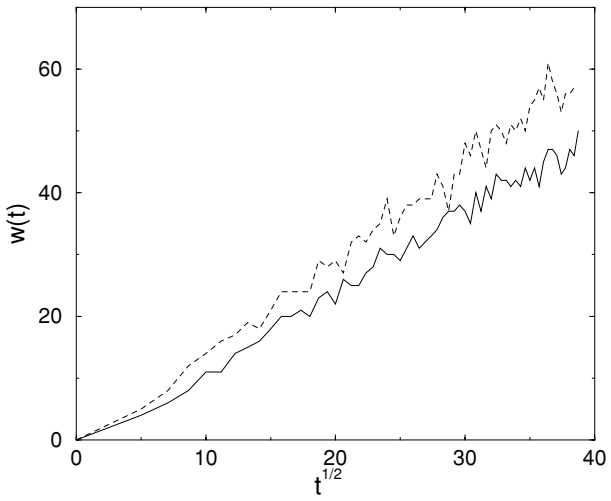

Figure 3. The average front size $w(t)$ of the stochastic (solid line) and CML (dashed line) models described in the caption of figure 2 plotted versus the square root of time. See the text for the definition of $w(t)$.

2.2. Further simplifications of the stochastic models

Even if the quantitative agreement between the stochastic and the CML models depends on the numerical precision in the determination of the probability distribution $R(u_i, r_i)$, we have observed that drastic approximations (such as a flat distribution between 0 and 1 or a δ-like Dirac distribution centred around a proper value) can be assumed without changing the qualitative behaviour of the stochastic model. Therefore, we have decided to simplify it by taking a δ-like distribution for R, with $r_i(t) = 1$. Moreover, in order to get rid of unnecessary technical complications, we have posed $b = a < 1$. Note that, having chosen $r_i(t) = 1$, this choice for b is consistent with avoiding the appearance of the fictitious fixed point $u_i = 1$. From now on we study the model

$$\begin{aligned}
&\tilde{u}_i(t) = (1-\varepsilon)u_i(t) + \frac{\varepsilon}{2}u_{i+1}(t) + \frac{\varepsilon}{2}u_{i-1}(t) \\
&u_i(t+1) = \begin{cases} 1 & \text{w.p.} \quad p = a\tilde{u}_i(t) \\ a\tilde{u}_i(t) & \text{w.p.} \quad 1-p \end{cases} \qquad \text{if} \quad \tilde{u}_i(t) > \Delta \\
&u_i(t+1) = \begin{cases} \tilde{u}_i(t)/\Delta & \text{w.p.} \quad p = a\Delta \\ a\tilde{u}_i(t) & \text{w.p.} \quad 1-p \end{cases} \qquad \text{if} \quad \tilde{u}_i(t) \leqslant \Delta .
\end{aligned} \tag{9}$$

that we call the *continuous stochastic model* (CSM). In the limit $\Delta \to 0$, it will be named the *discontinuous stochastic model* (DSM).

Thanks to the above simplifications, the transition from the chaotic/unsynchronized phase to the ordered/synchronized one is controlled by a single parameter, i.e. the contraction factor a.

3. The zero-dimensional case

The most important problem of linearly stable chaos is to understand how finite perturbations can propagate in spite of the average local contraction. To clarify this point, in this section we study model (9) in the limit $\varepsilon \to 0$, i.e. the zero-dimensional case. We show that, even

if 'chaotic' motion cannot be sustained whenever the Lyapunov exponent is negative, the non-uniform contraction induces non-trivial properties anyhow.

Our first observation concerns the probability $P(t, u(0))$ for a finite-amplitude perturbation $u(0)$ to never be amplified by the instability mechanism over a time t. In the DSM, such a probability can be easily factorized as

$$P(t, u(0)) = \prod_{n=1}^{t}(1 - u(0)a^n) \stackrel{t\to\infty}{\longrightarrow} \exp\left[-\sum_{k=1}^{\infty}\frac{(u(0)a)^k}{k(1-a^k)}\right] := \tilde{P}(u(0)). \tag{10}$$

One can see that, for $t \to \infty$, $P(t, u(0))$ approaches a finite value $\tilde{P}(u(0))$, that is both strictly larger than 0 and smaller than 1 for any value of $u(0)$, with $0 < a < 1$. The same conclusion can also be drawn for the CSM, although the algebra is more complicated in that case. The inequality $\tilde{P}(u(0)) > 0$ indicates that occasional amplifications are not strong enough to prevent the eventual absorption of the perturbation (this is consistent with our goal to deal with linearly stable processes). On the other hand, the inequality $\tilde{P}(u(0)) < 1$ indicates that the amplification process cannot be neglected. Notice that, since this holds true independently of $u(0)$ (although $\tilde{P}(u(0)) \to 1$ for $u(0) \to 0$), there is a difference with the convergence to a stable fixed point in a topologically chaotic map (e.g., think of the logistic map in one of the stability windows that follow the first period doubling) since, in that case, there would be a threshold (corresponding to the border of the basin of attraction) below which a monotonic contraction would start. A closer similarity exists with the so-called strange non-chaotic attractors, as they are characterized by a non-monotonic contraction even arbitrarily close to the attractor [18, 19].

The multifractal theory [20] provides the most appropriate framework to characterize this system. By following this approach, devised with reference to infinitesimal perturbations, we define the exponential growth rate of a finite perturbation $u(0)$:

$$\lambda(t, u(0)) = \frac{1}{t}\ln\left(\frac{u(t)}{u(0)}\right). \tag{11}$$

In the limit of infinitesimal perturbations ($u(0) \to 0$) $\lambda(t, u(0))$ is equivalent to the usual finite-time Lyapunov exponent [21]. The corresponding probability distribution is given by the relation

$$\mathcal{P}(\lambda, t, u(0)) = Q(t, u)\frac{\mathrm{d}u}{\mathrm{d}\lambda} \tag{12}$$

where $Q(0, u) = \delta(u - u(0))$ while λ and u are related by equation (11).

The multifractal spectrum is finally defined as

$$h(\lambda) = \lim_{t\to\infty}\lim_{u(0)\to 0}\left[\frac{1}{t}\ln\mathcal{P}(\lambda, t, u(0))\right]. \tag{13}$$

Since, for the aim of this paper, we are interested in studying the behaviour of finite perturbations, we avoid taking the $u(0) \to 0$ limit, thus introducing what we call a finite-size multifractal spectrum

$$H(\lambda) = \lim_{t\to\infty}\left[\frac{1}{t}\ln\mathcal{P}(\lambda, t, u(0))\right] \tag{14}$$

where the dependence on $u(0)$ disappears, since a shift in the initial condition gives rise to a correction that vanishes in the $t \to \infty$ limit. It is this trivial, but remarkable, property that makes $H(\lambda)$ a well defined quantity. In the following we show that it differs from the standard multifractal spectrum $h(\lambda)$, and that, therefore, even the zero dimensional system reacts differently to infinitesimal and finite perturbations over finite timescales. In the following, we determine $h(\lambda)$ and $H(\lambda)$ in both stochastic models.

3.1. Linear analysis

We start from the CSM, as the DSM is nothing but a limit case of the former one. The linear approximation amounts to assuming $u_i(t) < \Delta \; \forall i, t$. Recalling that $a < 1$ and $\Delta < 1$, standard combinatorial analysis implies

$$h_\Delta(\lambda) = \frac{\ln(\Delta)+\lambda}{\ln(a\Delta)}\left[\ln(1-a\Delta) - \ln\left(\frac{\ln(\Delta)+\lambda}{\ln(a\Delta)}\right)\right] + \frac{\ln(a)-\lambda}{\ln(a\Delta)}\ln\left[\frac{a\Delta\ln(a\Delta)}{\ln(a)-\lambda}\right] \qquad \ln a < \lambda \leqslant 0 \tag{15}$$

where we have made explicit the dependence on the parameter Δ. In the limit $\Delta \to 0$, the above expression reduces to

$$h_0(\lambda) \equiv \lim_{\Delta\to 0} h_\Delta(\lambda) = \ln(a) - \lambda. \tag{16}$$

On the other hand, performing the limit $\Delta \to 0$ before the limit $t \to \infty$ would yield the trivial result $h_\Delta(\lambda) = 0$, with the support of h_0 restricted to the point $\lambda = \ln a$. Thus, the non-commutativity of the limits $\Delta \to 0$ and $t \to \infty$ reveals that the discontinuous case is a singular limit of the CSM. In other words, the multifractal spectrum of the discontinuous model depends on the way it is defined. In all cases where the discontinuity is the idealization for a large but finite slope, it is obviously more meaningful to first take the limit $t \to \infty$. In any case, both ways of reasoning assume dealing with infinitesimal perturbations. In section 3.2 we shall see how the inclusion of finite perturbations leads to more significant modifications of the multifractal spectrum.

3.2. Non-linear analysis

Without loss of generality, we now consider a finite perturbation $u(0) = 1$ in the DSM. From equation (11) we see that $\lambda(t, u(0))$ is uniquely determined by the knowledge of $u(t)$ and $u(0)$. Accordingly, the knowledge of $\mathcal{P}(\lambda, t, u(0))$ is fully equivalent to that of the single-site probability distribution $Q(t, u)$, together with the initial condition

$$Q(0, u) = \delta(u - 1). \tag{17}$$

It proves useful to introduce the notation $u = a^n$ where n is a positive integer. Equation (11) can be rewritten as

$$\lambda(t, n) = \frac{n}{t}\ln a. \tag{18}$$

It implies that for $t \to \infty$, λ is bounded between $\ln a$ and 0.

Two possibilities are in order: either the system after time t has never been 'kicked' (i.e. it has never been reset to 1 by the instability mechanism) in which case the initial value has been contracted t-times by a factor a, or it has received at least one kick, thus losing memory of the initial condition. In the former case, occurring with probability $P(t, 1)$, $\lambda(t) = \ln a$. In the latter case, $\lambda(t) > \ln a$ and the accessible values of n are restricted to positive integer numbers strictly smaller than t (since the maximum possible contraction factor in t timesteps is a^t). Accordingly, n can be interpreted as the elapsed time since the last kick, and the probability distribution $Q(t, u)$ can be factorized as the product of the probability $G(t - n)$ of receiving a kick at time $t - n$ times the probability $P(n, 1)$ of not being kicked anymore for the remaining n timesteps,

$$Q(t, n) = G(t - n)P(n, 1). \tag{19}$$

In appendix, we show that $G(t) \approx \exp(-\nu_c t)$, where ν_c is implicitely determined by equation (A5). Accordingly,

$$H(\lambda) = -\nu_c\left(1 - \frac{\lambda}{\ln a}\right) \tag{20}$$

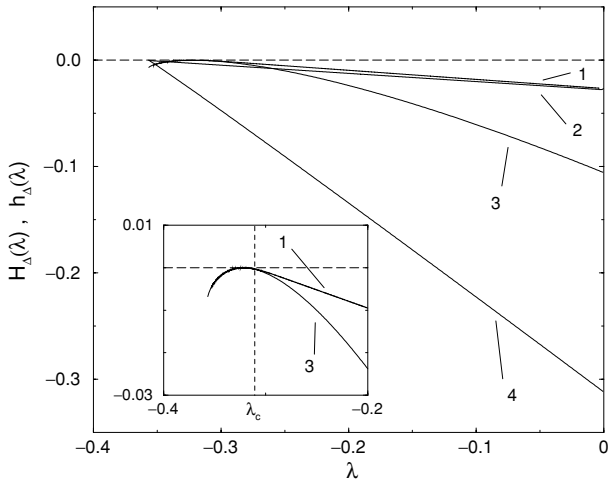

Figure 4. Probability distributions of the exponential growth rate (11) in the large time limit for the stochastic model (9) in the zero-dimensional case, with $a = 0.7$. Lines 1 and 3 refer to the continuous case ($\Delta = 0.0097$), with a finite size or an infinitesimal initial perturbation, respectively, while lines 2 and 4 refer to the discontinuous case ($\Delta \to 0$), still with a finite size or infinitesimal initial perturbation, respectively. The deviation from a straight line of curve 2 is due to finite time effects. In the inset the difference between curves 1 and 3 is magnified.

since the contribution arising from $P(n, 1)$ is negligible in the limit $t \to \infty$. This implies that the multifractal spectrum is defined in the open interval $(\ln a, 0)$, where it has a linear shape. Moreover, one can see from equation (A5) that the slope $v_c / \ln a$ increases monotonically from -1 (for $a \to 0$) to 0 (for $a \to 1$).

Curves 2 and 4 in figure 4 correspond to the non-linear and linear analysis of the DSM, respectively with $a = 0.7$. The latter curve lies well below the former one, indicating that the linear analysis leads to an underestimation of the fluctuations. This is a general fact holding for all values of a in the meaningful range (0, 1). The difference must be attributed to the sporadic amplifications due to the discontinuity.

It is now important to test whether the difference between linear and non-linear curves also persists when the discontinuity is removed, i.e. in the CSM. For the sake of simplicity, we fix Δ equal to $a^{\bar{n}}$ and suppose that $\bar{n}$ is a non-negative integer, so that $u(t)$ is defined on a discrete subset of the unit interval, $\{a^n\}_{n=0,1,\ldots}$. This assumption does not affect the main conclusions, while it allows one to write a simple recursive equation for the probability distribution $Q(t, n)$:

$$\begin{aligned} Q(t+1,0) &= \sum_{k=0}^{\bar{n}} Q(t,k)\, a^{k+1} \\ Q(t+1,n) &= \begin{cases} (1-a^n)Q(t,n-1) + a^{\bar{n}+1} Q(t,n+\bar{n}) & 0 < n \leqslant \bar{n} \\ (1-a^{\bar{n}+1})Q(t,n-1) + a^{\bar{n}+1} Q(t,n+\bar{n}) & n > \bar{n}. \end{cases} \end{aligned} \tag{21}$$

Equations (21), with the initial condition $Q(0, n) = \delta_{n,0}$ and boundary conditions $Q(t, n) = 0 \; \forall \, t > n$, can be numerically iterated to obtain the finite-size multifractal distribution in the continuous case.

Since the development of analytical techniques to determine H_Δ is by far more complex than in the previous case, we have limited ourselves to determining the multifractal spectrum numerically. The linear and non-linear spectra are reported in figure 4 for $\Delta = 0.0097$ (curves 3 and 1, respectively). There, we can see that the non-linear curve lies well above the standard multifractal spectrum, indicating that it is not the discontinuity which is responsible for the

difference between the behaviour of infinitesimal and finite-size perturbations. Moreover, the overall closeness of curves 1 and 2 reveals that the removal of the discontinuity does not introduce significant differences in the finite-size spectrum.

Finally, let us closely compare $H_\Delta(\lambda)$ with $h_\Delta(\lambda)$: the inset in figure 4 reveals the existence of a critical value λ_c (see the dashed line) separating the left-hand region where the two spectra coincide, from the right-hand one where h_Δ decreases faster than H_Δ. According to thermodynamic formalism, the linear dependence of H_Δ on λ above λ_c is suggestive of a phase transition between a perturbative regime, correctly described by the linear analysis, and a 'non-linear response' regime, where the role of finite perturbations cannot be neglected. A more refined analysis would be worthwhile, but it would go beyond the aims of the present paper.

4. The spatially extended case

The past study of stable chaos has revealed that, as long as finite chains are considered, no qualitative difference exists with standard stable systems. After an exponentially long transient, a periodic behaviour is always attained. As remarked in section 2, a similar scenario is indeed exhibited by our stochastic models.

Equation (10) shows that in the absence of spatial coupling, there is a finite probability $\tilde{P}(u(0))$ for an initial perturbation $u(0)$ to be contracted for an infinite amount of timesteps and thus of being effectively absorbed. It is worth defining here:

$$u_M(t) = \max_i u_i(t). \tag{22}$$

In particular, this allows us to apply the above reasoning to the coupled case, with $u_M(0)$ playing the role of $u(0)$; the probability $\tilde{P}$ that an arbitrary, spatially extended, perturbation is contracted forever on every site i satisfies the inequality

$$\tilde{P}(u_1, u_2, \ldots, u_L) \geqslant \left[\prod_{n=1}^{\infty}(1 - u_M(0)a^n)\right]^L = \left[\tilde{P}(u_M(0))\right]^L \tag{23}$$

where $\tilde{P}(u_M(0))^L$ is small but finite for every finite lattice length L. Thus, the average time τ needed for any perturbation to die out (i.e. to be contracted below some arbitrarily small threshold value) is finite and does not grow faster than exponentially with the system size

$$\tau \leqslant \left[\tilde{P}(u_M(0))\right]^{-L}. \tag{24}$$

In the active (i.e. chaotic) phase where perturbations propagate with a finite velocity, τ grows exponentially with L, since the only way for a perturbation to die out is to be contracted in all sites, while in the inactive phase, the latter is only a sufficient condition and not a necessary one, and perturbations die out on significantly shorter timescales.

At variance with the zero-dimensional case, direct numerical simulations of the DSM in a 1-d lattice reveal the existence of a regime where finite perturbations self-sustain. This is clearly shown in figure 6, where we have reported the spacetime and ensemble average value m of the perturbation for different values of the contraction rate a. Above $a = 0.60(5)$, non-zero amplitudes are actually observed. It is, therefore, crucial to understand the reason why the spatial interactions can stabilize finite perturbations in spite of the diffusive nature of the coupling.

The natural extension of what we have learnt in zero-dimensions consists in looking at the joint probability distribution $Q_J(t, u_1, u_2, \ldots, u_L)$ over the whole lattice. If the system is sufficiently above the transition to stable chaos, it seems reasonable, in a first approximation,

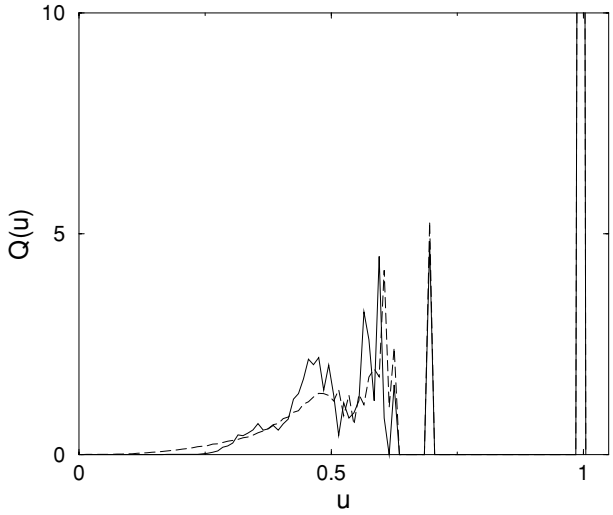

Figure 5. Stationary, single-site probability distribution $Q(u)$ for $a = 0.7$ and $\Delta = 0.01$ computed by numerical simulation of the CSM (dashed line) and by numerical solution of equation (26) for $N = 3$ (solid line). Both distributions have been obtained subdividing the unit interval into 100 channels. The δ-peak in $u = 1$ has been cut to magnify all other details.

to neglect spatial correlation. This is certainly incorrect for those sites that are close to propagating fronts, but the fraction of such lattice sites is definitely negligible. Accordingly, we approximate the joint probability distribution as a product of single-site probabilities $Q(t, u)$:

$$Q_J(t, u_1, u_2, \ldots, u_L) \approx Q(t, u_1)Q(t, u_2)\cdots Q(t, u_L). \tag{25}$$

Within this approximation, the single-site probability distribution corresponding to the stochastic dynamics (9) satisfies the following Frobenius–Perron equation:

$$\begin{aligned} Q(t+1, u) = {} & g(u) \int_0^\infty \prod_{i=1}^N \mathrm{d}v_i \; Q(t, v_i)\, \delta\left(u - \frac{a}{N}\sum_{i=1}^N v_i\right) \\ & + a\Delta \int_0^\infty \prod_{i=1}^N \mathrm{d}v_i \; Q(t, v_i)\, \delta\left(u - \frac{1}{N\Delta}\sum_{i=1}^N v_i\right) \\ Q(t+1, 1) = {} & \int_{a\Delta}^\infty \mathrm{d}u\, u \int_0^\infty \prod_{i=1}^N \mathrm{d}v_i \; Q(t, v_i)\, \delta\left(u - \frac{a}{N}\sum_{i=1}^N v_i\right) \end{aligned} \tag{26}$$

where δ is the Dirac distribution, v_i is the amplitude of the perturbation in the ith neighbouring site, N is the number of democratically coupled sites (for later convenience we leave N unspecified—note that $N = 3$ in a one-dimensional lattice with nearest neighbour coupling) and

$$g(u) = \begin{cases} 1 - u & \Delta < u < 1 \\ 1 - a\Delta & 0 \leqslant u \leqslant \Delta \end{cases}.$$

It is easy to verify that the support of the single-site probability distribution $Q(t, u)$ remains confined to the unit interval, provided that this holds true for the initial condition as well.

In figure 5 we have plotted the single-site probability distributions obtained by directly iterating the stochastic model and the approximate Frobenius–Perron equation (26) (solid and

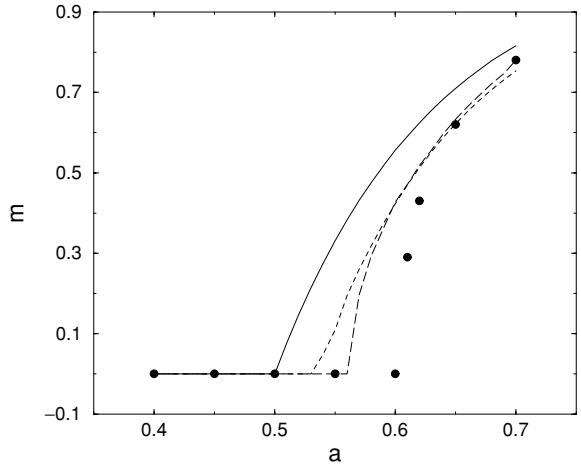

Figure 6. The spacetime and ensemble average value m of the perturbation $u_i(t)$ as a function of the contraction rate a. The dots refer to the result of numerical simulations with lattices of size $L = 1000$; the solid, dashed and long-dashed curves refer to the mean-field analysis, Gaussian approximation ($N = 3$) and the numerical integration of the Frobenius–Perron equation (26), respectively.

dashed lines, respectively). The reasonable overlap confirms the validity of the factorization hypothesis (at least away from the critical region). Quite unexpectedly, spatial correlation (neglected in equation (26)) induces a smoother distribution. However, the mean value, equal to 0.773 in the direct simulations, is very close to 0.770, the value obtained by the iteration of the Frobenius–Perron operator, and a good agreement is found also for the variances that are respectively equal to 0.063 and 0.061.

For $N = 1$ (no coupling), equation (26) corresponds to the zero-dimensional dynamics discussed in the previous section, and the evolution equation is exact. It reduces to the linear equation

$$\begin{aligned} Q(t+1,u) &= g(u)\frac{1}{a}Q\left(t,\frac{1}{a}u\right) + a\Delta^2 Q(t, a\Delta u) \\ Q(t+1,1) &= a\int_{\Delta}^{\infty} \mathrm{d}u\, u\, Q(t,u). \end{aligned} \tag{27}$$

The only fixed point of this equation is $Q(t,\ u) = \delta(u)$, i.e. the absorbing state. The multifractal spectrum discussed in section 3 is nothing but a sophisticated characterization of the convergence towards such a fixed point.

On the opposite side of the zero-dimensional limit, there is the mean-field approximation that corresponds to the limit $N \to \infty$. In this limit, statistical fluctuations vanish and the dynamics reduces to the evolution of the mean value $m(t) = \int \mathrm{d}u\, Q(t,u)u$, that reads

$$m(t+1) = \begin{cases} m(t)[2a - a^2 m(t)] & \text{if} \quad m(t) > \Delta \\ m(t)[2a - a^2\Delta] & \text{if} \quad m(t) \leqslant \Delta. \end{cases} \tag{28}$$

For $a < a_c = (1 - \sqrt{1-\Delta})/\Delta$, equation (28) displays the stable fixed point $m_1 = 0$. This is the same regime found in zero-dimensions and corresponds to the eventual absorption of any initially finite difference. Increasing a above a_c, the system undergoes a bifurcation: m_1 becomes unstable and a second (stable) fixed point $m_2 = (2a-1)/a^2$ appears. In the discontinuous limit ($\Delta \to 0$)$a_c \to 1/2$. In figure 6 the predictions of the mean-field approach

are compared with the results of direct simulations. We see that, in spite of the approximations, there are no severe differences; the critical point is underestimated by approximately 17%.

Mean-field analysis represents the first approximation of the evolution operator Q. The numerical results reported in figure 5 suggest that one can approximate Q as the sum of a δ contribution plus a Gaussian

$$Q(t, v) = A_t \delta(v - 1) + \frac{1 - A_t}{\sqrt{2\pi V_t}} \exp\left[-\frac{(v - \bar{v}_t)^2}{2V_t} \right]. \tag{29}$$

This allows us to derive three evolution equations for the variables A_t, $\bar{v}_t$ and V_t, whose solution is reported in figure 6 (see dashed curve). A comparison with the other curves reveals both an improvement over the mean-field approach (the critical value has increased to $a_c = 0.536$) and that the Gaussian approximation captures the essence of the dynamics in the absence of spatial correlation (see the long-dashed curve resulting from the iteration of the simplified Frobenius–Perron equation (26)).

For Δ larger than 0, we observe just a slight shift of the critical value: no qualitatively new phenomena are induced by the continuity of the model.

Finally, we wish to comment on the role of ε. At variance with the zero-dimensional case, we obviously expect the coupling to play some significant role. Indeed, numerical simulations show that the transition point depends on the actual value of ε and, more specifically, that deviations from the democratic coupling lower the value of the order parameter. Anyway, from an analytical point of view, even a simple mean-field approach becomes immediately non-trivial, as it is no longer possible to write down a a single closed equation for the average value of u_i.

5. Open problems and conclusions

In this paper, we have shown that a simple *stochastic* model, specifically designed to simulate a different response to finite and infinitesimal perturbations, is able to capture the key features of irregular behaviour in linearly stable systems. In particular, we have seen that replacing the sequence of jumps generated by the CML dynamics with a genuine stochastic process allows for a faithful reconstruction of the front propagation. The main theoretical advantage of the stochastic model is the disentanglement between the generation of a pseudo-random pattern and the evolution of perturbations. In reality the two issues are interlaced. Their separation has allowed us to clarify under which conditions finite perturbations can be effectively sustained throughout an infinite lattice. In particular, full consistency exists between the CML and the stochastic models in the chaotic regime, since we can state that the amplification of finite perturbations contributes to sustaining an irregular regime.

On the other hand, the transition to the ordered phase observed in the CSM/DSM models does not reproduce the analogous behaviour displayed by the CML. In the latter case, it was observed that the critical region is not point-like, but rather extended to what has been called a 'fuzzy region', where ordered and chaotic dynamics alternate in a quite irregular manner [14]. The reason for the difference is that in the CML model the absence of local chaos makes the sequence of multipliers increasingly less random in the transition region. In the stochastic model, instead, the randomness of multipliers is always assumed *a priori*. In spite of such a difference, it is nevertheless instructive to note that a transition persists without modifying the stochasticity in real space.

A more precise analogy for the transition investigated in the previous section is provided by the correspondence with the problem of synchronization in the presence of external noise. In fact, in this latter context, the noise represents the (unavoidable) source of stochasticity

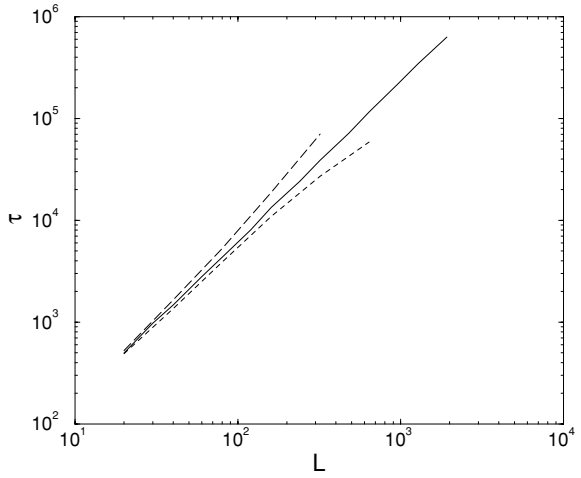

Figure 7. Log–log plot of the absorption time τ as a function of the system size L in the continuous case ($\Delta = 0.01$) near the critical value for different control parameter values: $a = 0.6051$ (dashed line), $a = 0.655$ (solid line) and $a = 0.6061$ (long-dashed line).

in the synchronous as well as in the asynchronous regime. A recent numerical study of the synchronization transition in linearly stable systems suggests that it belongs to the universality class of directed percolation (DP) [15]; it is tempting to verify whether the same holds true in our stochastic models.

As already mentioned, even though the front velocity v_F is a good order parameter to characterize the transition, it is quite difficult to obtain a reliable estimate of the critical value of the control parameter a_c from the vanishing of v_F. In fact, finite-size corrections and transient effects, combined with the existence of wild fluctuations, prevent a careful analysis. A more efficient method amounts to measuring the dependence of the so-called *absorption time* τ on the system size L. This is defined as the time required for the space-averaged perturbation $\bar{u}(t)$ to become smaller than some very small but finite threshold Γ. Fluctuations of τ can be efficiently reduced by averaging over a sufficiently large ensemble of initial conditions. In the active phase, τ is expected to diverge exponentially with L (stable chaotic regime), while in the absorbing phase, it should depend, at most, logarithmically on L. Only at the critical point, τ exhibits a power-law dependence

$$\tau(L, a_c) \sim L^z \tag{30}$$

where $z = \nu_\parallel/\nu_\perp$ is the so-called dynamical exponent and $\nu_\parallel$ and $\nu_\perp$ represent the critical exponents associated with space and time correlation lengths, respectively. We have performed numerical simulations for both the CSM (with $\Delta = 0.01$) and DSM, averaging over 3000 realizations of the stochastic process and over randomly sampled initial conditions. In the CSM we find $a_c = 0.6055\ldots$, with $z = 1.58 \pm 0.02$; in the DSM we obtain $a_c = 0.6065\ldots$ and $z = 1.56 \pm 0.06$. The errors have been estimated as the maximum deviation from linearity in the log–log plot that has been used for extracting the scaling law (30) (see, for instance, figure 7, where τ has been plotted versus L for $\Delta = 0.01$ and different values of a). These results agree with the most accurate numerical estimates of the DP value, $z = 1.5807$ [22].

We also measured the critical exponent δ, associated with the temporal decay of the density of active sites $\rho(t)$, i.e. those sites where $u_i(t) > \Gamma$: at the critical point, $\rho(t)$ is characterized by the scaling law

$$\rho(t, a_c) \sim t^{-\delta} \tag{31}$$

where $\delta = \beta/\nu_\parallel$ and β is the critical exponent associated with the order parameter. By averaging over 3000 realizations and choosing a sufficiently large value of L to get rid of finite-size corrections, we have found $\delta = 0.150 \pm 0.01$ for the CSM and 0.155 ± 0.005 for the DSM, to be compared with the DP value $\delta = 0.1595$ [22].

Altogether, our simulations support the hypothesis that the transition belongs to the same universality class as DP. This may look an almost trivial result, since local spreading is the only mechanism for the propagation of perturbations (or, in different language, active sites, infections). However, the whole problem is definitely more subtle, as an absorbing state cannot be identified so clearly. In fact, we have already seen that the determination of the absorption time requires fixing a somehow arbitrary threshold Γ, and the same is true for the computation of the active sites at a given time. Even though we have found that our results are independent of the choice of Γ (provided it is small enough), this may appear as a numerical trick. In principle, in an infinite system, no matter how small a perturbation is, there is always some finite probability that it gives rise to a burst. This seems contrary to the existence of a truly absorbing state. On the other hand, in section 4 we have argued that in a finite chain any perturbation eventually dies out. This in practice amounts to the existence of an absorbing state. The smaller u_M is, the more likely it is that the perturbation keeps being absorbed; in this case any perturbation $w_i(t)$ has a finite probability to enter an infinite 'contraction loop', in which every site i is monotonically contracted for any time larger than t.

It would be nice to put our qualitative arguments on a more rigorous basis, by defining a suitable finite-size Lyapunov exponent that is negative below some threshold to indicate that $u^* = 0$ is a truly absorbing state. However, it is not clear whether this could be accomplished, since we know that in the chaotic phase the fixed point $u^* = 0$ should be at the same time 'macroscopically' unstable, since perturbations eventually drive the system towards the only stable state, and 'microscopically' stable, to mean that small enough perturbations have to be absorbed. In the future, we hope to be able to clarify whether it is possible to define an indicator that contains both messages.

Acknowledgments

RL and AP wish to thank R Kapral for early discussions about a meaningful definition of the stochastic model. A Pikovsky, V Ahlers and A Torcini are acknowledged for useful exchanges of ideas about the characterization of the transition. A profitable discussion on the zero-dimensional model has been carried on with Y Elskens. We would also like to thank the anonymous referee for having suggested the solution method reported in the appendix. Part of this work has been completed thanks to the financial support of the NATO contract CRG.973054. We also thank ISI in Torino, where part of this work was performed.

Appendix. Multifractal distribution

In this appendix we show that $G(t)$ decays exponentially. The last time T when $u(T) = 1$ can be expressed as the sum of i.i.d. random variables,

$$T = \sum_{i=1}^{I} \tau_i$$

where τ_i is the interval between two consecutive returns to 1 and I is the fluctuating number of returns. By denoting the return probability after a time τ with $P_r(\tau)$, it is readily seen that

$$P_r(\tau) = \frac{a^\tau}{1-p}\prod_{i=1}^{\tau-1}(1-a^i) \tag{A1}$$

where $p \equiv \tilde{P}(1)$ (see equation (10)) is the probability of never returning to 1. Moreover, the probability $P_1(I)$ for a generic trajectory to return I times to 1 is

$$P_1(I) = (1-p)^I p. \tag{A2}$$

Let us now introduce the expectation value

$$\phi(\nu) \equiv \langle \exp(\nu\tau)\rangle = \sum_{\tau=1}^{\infty} P_r(\tau)\exp(\nu\tau) \tag{A3}$$

where the sum over τ is extended to infinity as we are interested in the asymptotic dynamics. The mutual independence of the random variables τ_i allows writing

$$\sum_{T=1}^{\infty}\exp(\nu T)G(T) \equiv \langle \exp(\nu T)\rangle = \sum_{I=0}^{\infty}\phi(\nu)^I P_1(I). \tag{A4}$$

From the definition (A2), it follows that the above expression is finite for $\nu < \nu_c$, where ν_c is defined by the equation $\phi(\nu_c)(1-p) = 1$. This implies that $G(t)$ decays exponentially with the rate ν_c. The explicit expression defining ν_c is

$$\sum_{\tau=1}^{\infty}\exp(\nu_c\tau)\prod_{I=1}^{\tau-1}(1-a^I)a^\tau = 1. \tag{A5}$$

References

[1] Eckmann J-P and Ruelle D 1985 *Rev. Mod. Phys.* **67** 617
[2] Kaneko K 1984 *Prog. Theor. Phys.* **74** 1033
[3] Livi R, Politi A and Ruffo S 1986 *J. Phys. A: Math. Gen.* **19** 2033
[4] Grassberger P 1989 *Phys. Scr.* **40** 346
[5] Wolfram S ed 1986 *Theory and Applications of Cellular Automata* (Singapore: World Scientific)
[6] Crutchfield J P and Kaneko K 1988 *Phys. Rev. Lett.* **60** 2715
[7] Livi R, Martinez-Mekler G and Ruffo S 1990 *Physica D* **45** 452
[8] Politi A, Livi R, Oppo G L and Kapral R 1993 *Europhys. Lett.* **22** 571
[9] Kapral R, Livi R, Oppo G L and Politi A 1994 *Phys. Rev.* E **49** 2009
[10] Cuche Y, Livi R and Politi A 1997 *Physica* D **103** 369
[11] Kapral R, Livi R and Politi A 1997 *Phys. Rev. Lett.* **79** 2277
[12] Livi R, Ruffo S and Politi A 1992 *J. Phys. A: Math. Gen.* **25** 4813
[13] Cecconi F and Politi A 1999 *J. Phys. A: Math. Gen.* **32** 7603
[14] Cecconi F, Livi R and Politi A 1998 *Phys. Rev.* E **57** 2703
[15] Baroni L, Livi R and Torcini A 2001 *Phys. Rev.* E at press
[16] Domany E and Kinzel W 1984 *Phys. Rev. Lett.* **55** 311
For a recent review see Grassberger P 1997 Directed percolation: results and open problems *Nonlinearities in Complex Systems, Proc. 1995 Shimla Conf. on Complex Systems* ed S Puri *et al* (New Delhi: Narosa)
[17] Politi A and Torcini A 1994 *Europhys. Lett.* **28** 545
[18] Pikovsky A and Feudel U 1995 *Chaos* **5** 253
[19] Feudel U, Kurths J and Pikovsky A 1995 *Physica* D **88** 176
[20] Beck C and Schlögl F 1993 *Thermodynamics of Chaotic Systems* (Cambridge: Cambridge University Press)
[21] Paladin G and Vulpiani A 1987 *Phys. Rep.* **156** 147
[22] Jensen I 1996 *J. Phys. A: Math. Gen.* **29** 7013
Jensen I 1999 *Preprint* cond-mat/9906036